Field and Technical Report

MICROFOCUS X-RAY TOMOGRAPHY AS A METHOD FOR CHARACTERISING MACRO-FRACTURES ON QUARTZ BACKED TOOLS

JUSTIN PARGETER[1,2]*, LUNGA BAM[3], FRIKKIE DE BEER[2,3] & MARLIZE LOMBARD[2]

[1]*Interdepartmental Doctoral Program in Anthropological Sciences, Stony Brook University, Stony Brook, NY, USA*
(*Corresponding author. E-mail: justin.pargeter@gmail.com)

[2]*Centre for Anthropological Research & Department of Anthropology and Development Studies, University of Johannesburg, Auckland Park, 2006, South Africa*

[3]*Radiation Science, South African Nuclear Energy Corporation (Necsa), Pretoria, South Africa*

ABSTRACT

Here we present the first assessment of microfocus X-ray tomography (micro-XCT) as an analytical technique to generate data about macro-fractures on small quartz backed tools similar to those currently held to represent the oldest known evidence for bow hunting. Our experimental results are derived from 21 replicated quartz backed tools randomly selected from a population (n = 218) that were broken in a controlled hunting context. We used 3D data obtained from micro-XCT scans to identify macro-fractures and to derive more accurate measurements for these fractures. Our results demonstrate that the micro-XCT technique overcomes reflected-light challenges associated with analysing quartz through conventional macro-fracture approache s. We were able to increase the total observed macro-fracture sample by 33% compared with conventional approaches using a hand-lens. Whereas macro-fracture data could be refined, the additionally gained data did not change interpretations obtained from a conventional macro-fracture analysis. It did, however, marginally change the degree of significance in differences between the different applications. During this study, we also detected micro-fracture features, such as possible fracture wings and microscopic linear impact traces (MILTs). With further studies, the morphometric traits of these micro-fracture features could be useful for distinguishing between ancient weapon-delivery systems.

Keywords: hunting weaponry, Micro-XCT scanning, macro-fractures, quartz, backed tools.

INTRODUCTION

The antiquity of hunting technology is a key question in Pleistocene archaeology (see Iovita & Sano 2016 and references therein). Estimates for the emergence of mechanically-projected weaponry such as spear throwers, darts and/or bows and arrows currently range between 10–15 ka to more than 100 ka (Lombard & Phillipson 2010). The variability and complex patterning among ethnographic hunting weapons suggests that a simple answer to the question of where and when these weapon systems emerged is unlikely. Moreover, the diagnostic components of ethnographic bows and arrows, spear throwers and darts are their highly perishable organic components. Much of the Pleistocene record lies beyond the preservation remits of these materials, making the identification and distinction of weapons and specific weapon 'types' based on organic remains difficult.

We explore microfocus X-ray Computed Tomography (micro-XCT) as a new method that could add to the existing toolkit for generating increasingly robust functional interpretations for the stone components of hunting weapons. Many functional studies of stone artefacts focus on the morphometric traits of stone artefacts to diagnose weapon types (see Hutchings 2016 for synthesis). These techniques can be applied to assess the potential of artefact classes to function as projectile tips in quantitative terms (e.g. Sisk & Shea 2009), but they have produced ambiguous results, especially when retouched points are lacking from assemblages, or where non-pointed artefacts such as geometric backed pieces were potentially used as weapon components (e.g. Lombard & Pargeter 2008). Moreover, techniques based on the morphometric variation of artefacts tend to derive their criteria from measurements of ethno-historical weapons (mostly from North American contexts [e.g. Dockall 1997]), and not all pointed archaeological artefacts measured during such analyses were used as, or intended for, weapon tips (e.g. Phillipson 2009). Thus, there exists an interpretative shortfall in morphometric approaches to function, mostly because of the inability to test directly for the actual application of a tool (Lombard & Phillipson 2010).

Methods focused on artefact breakage patterns, fracture size, and the micro-fracture features within these breakages show potential for identifying prehistoric weapon components (for summaries/examples see Hutchings 2016; Iovita *et al.* 2016; Sano *et al.* 2016). However, a number of issues exist with the current macro- and micro-fracture methods. Macro-fractures are three-dimensional objects with complex micro-topographies and internal fracture features. Macro-fracture size is particularly prone to distortion at a two-dimensional level because their complex topographies are imprecise when viewed in two dimensions (2D). Recently, a number of papers have demonstrated the problems with current approaches to identifying and characterising macro-fractures in terms of fracture terminations, initiations, and the surfaces on which macro-fractures initiate (e.g. Pargeter 2013; Rots & Plisson 2013; Hutchings 2016).

Macro-fractures are especially difficult to identify and diagnose on minerals such as quartz. Quartzes are highly light reflective and generally anisotropic, making them notoriously difficult to analyse. However, the accurate identification of macro-fractures on quartz artefacts, potentially used as weapon components in the past, could add value to our interpretative repertoire. Our hypothesis is therefore that X-ray attenuation, which is also a function of the density and thickness of the material and manifests in a micro-XCT scan, instead of reflected light, should be able to overcome light-related issues associated with analysing fracture patterns that developed on quartz tools during their use-life. These factors contribute towards the challenges in identifying early arrow tips, which were likely made on quartz (Wadley & Mohapi 2008; Lombard 2011).

We report on a new method, specifically aimed at resolving some of the above mentioned technical challenges associated with fracture analyses, and at refining our ability to interpret potential impact use of quartz artefacts. We used micro-XCT to generate high-resolution 3D data on quartz backed tools, shot experimentally as spearheads, spear barbs, and arrowheads (Pargeter et al. 2016). Micro-XCT is a non-destructive radiation-based analytical technique, during which X-rays probe objects to reveal their physical internal and external structures in three dimensions (3D) and at high resolution (maximum spatial resolution of 200 μm) (Hoffman & De Beer 2012; Cnudde & Boone 2013). Micro-XCT systems also generate data with well-defined surface areas of the object, allowing for more accurate detection and analysis of artefacts and their fractures in 3D.

BACKGROUND TO THE MACRO-FRACTURE METHOD

Since the 1980s, multiple experimental projects have demonstrated that a distinct subset of macro-fracture types, known as diagnostic impact fractures (DIFs), can be associated with the hunting function of stone artefacts (see Eren *et al.* 2016 for synthesis). No universal size cut-off is typically employed to define a 'macro' *versus* 'micro' fracture. However, macro-fractures are typically studied with a hand-lens or low-powered microscope whereas micro-fractures require more powerful microscopes and scanning techniques. The method is based on principles derived from actualistic and laboratory-based experimentation, and from fracture-mechanics research in the material sciences. DIFs are interpreted as resulting from lateral impact events, and are thus usually, but not exclusively, associated with weapon use (Fischer *et al.* 1984; Lombard 2005). Four DIF types have been defined by their characteristic initiations and terminations: step-terminating bending fractures, spin-off fractures > 6 mm (on large tools), bifacial spin-off fractures, and impact burinations (Fischer *et al.* 1984). Unifacial spin-off fractures < 6 mm are included in our DIF results because many of our tools measured < 6 mm in breadth (Pargeter *et al.* 2016).

Rots & Plisson (2013) recently highlighted a number of issues with the current methods of macro-fracture analysis. They show that variations in how macro-fracture scars are identified, quantified, and described, have led to problems in inter-observer variability. There are currently a wide range of terms used to describe macro-fractures with no single agreed upon definitional set. One of the biggest problems in current macro-fracture research is the use of photographs to illustrate macro-fracture scars. There are currently no standardised protocols for such photographs with most arguments about the macro-fracture method revolving around whether those features depicted are in fact macro-fractures related to impact use such as hunting.

Even though single 'diagnostic' fractures guide some functional interpretations, it is the patterning of DIFs (i.e. the type, co-occurrence, relationship to retouch and ventral location), that is more informative when diagnosing ancient weaponry (Pargeter 2013; Rots and Plisson 2013). For example, experiments on quartz backed tools by Pargeter and colleagues (2016) found that DIF types, locations, and frequencies can be used to differentiate between the experimental arrowheads and hand-cast spearheads. These experiments also confirmed previous observations that link DIF size to weapon velocity, but that this observation is better represented by the comparison of fracture area in relationship to tool area than linear DIF size (e.g. length) (Pargeter *et al.* 2016). DIFs often occur as irregular shapes on tool surfaces, and measuring size along one axis only

(i.e. length) provides limited information about impact-scar morphology or area (Pargeter *et al.* 2016). Data generated with micro-XCT allows for both fracture morphology and 3D measurements of fracture area to be recorded with accuracy. These observations provide a backdrop to our current micro-XCT study.

SAMPLE AND METHODS

We selected a sample of 21 replicated quartz backed pieces randomly from a population of 218 tools that were broken in a controlled hunting context (Table 1; see Pargeter *et al.* 2016 for background to the experiments). The shooting experiments were projection-velocity controlled with a Beta Master Brand Chronometer, which allows for the testing of this variable as a factor in the formation of macro- and micro-fracture features. The tools were hafted transversely as spear- ($n = 75$) or arrow-heads ($n = 75$), or diagonally as barbs ($n = 68$); data for the barb category were not included in Pargeter and colleagues (2016) representing three functional populations (Fig. 1). They were fired at a suspended rack of pork ribs (without skin), at an average velocity of 28 m/s with a standard deviation of 0.94 m/s. This velocity corresponds with the lower end of the experimental bow spectrum and with estimates of *c.* 33 m/s for bows used by Kalahari hunter-gatherer groups in southern Africa (see Pargeter *et al.* 2016: table 2). The spears were hand-cast at an average velocity of 9 m/s with a standard deviation of 1.04 m/s.

After the experiments all the quartz backed tools were examined for macro-fractures following existing protocols that emphasise the use of a hand-lens and appropriate lighting (see Lombard 2005; Lombard & Pargeter 2008). Pargeter and colleagues (2016) employed a strict macro-fracture framework following the guidelines established by Fischer and colleagues (1984) and Geneste and Plisson (1990). These guidelines specify details of the initiation and termination of DIFs when referring to fracture patterns. All fractures were counted and assemblage-level statistical summaries of their occurrences were provided (see Pargeter *et al.* 2016: table 3).

We scanned the experimental artefacts with a NIKON XTH 225ST system at the Micro-focus X-ray Radiography/Tomography (MIXRAD) laboratory of the South African Nuclear Energy Corporation (Necsa) (Hoffman & De Beer 2012). This is a high-resolution system consisting of a tungsten target with a 3.7 μm spot size with a variable energy potential ~25 to 225 kV. The spatial resolution obtained through normal geometric enlargement of the sample for the 3D tomogram in this investigation is 0.006 μm^3. Each sample was scanned at a potential of 110kV and beam current of 55 uA to obtain adequate beam penetration > 10% from background and optimal image contrast. During the scan the sample rotated in equal angular steps through 360° to produce, for these samples, 1000 radiographs at each step angle which are then reconstructed using the CT-Pro 3D-reconstruction software (Hoffman & De Beer 2012). The reconstruction process transforms the acquired 2D radiographs into a virtual 3D volume, which is an exact digital copy of the sample. This virtual 3D volume was then analysed using VGStudioMAX™ (ver. 2.2) rendering software allowing for 3D rendering of the sample. Statistical comparisons of continuous variables were done using permutation tests comparing sample means. Categorical variables were compared using chi-square tests. All statistical tests were conducted using the R statistical platform.

RESULTS

Table 1 contains a detailed overview of the macro-fracture results recorded on the experimental quartz backed tools prior

TABLE 1. *Overview of macrofracture results from the Pargeter* et al. *(2016) experiments and the Necsa 3D scanning. Note that one tool can have more than one macrofracture. UF: unifacial; BF: bifacial.*

Data source		Arrowhead n = 75		Spearhead n = 75		Spear barb n = 68		Chi-square results
		n	%	n	%	n	%	
Pre-Necsa	Step terminating	37	37.76	29	21.17	7	12.3	Chi-sq = 49.53, d.f. = 7, *P*-value < 0.0001
	BF spin-off	2	2.04	14	10.22	0	0.0	
	UF spin-off < 6 mm	4	4.08	7	5.11	7	12.3	
	UF spin-off > 6 mm	1	1.02	18	13.14	0	0.0	
	Impact burination	6	6.12	18	13.14	3	5.3	
	Hinge/feather term.	1	1.02	0	0.00	4	7.0	
	Notch	20	20.41	13	9.49	8	14.0	
	Snap	20	20.41	37	27.01	22	38.6	
	Tools with DIF	**34**	**45.3**	**55**	**73.3**	**17**	**25.0**	
	Ventral DIF	**45**	**77.6**	**57**	**66.3**	**15**	**22.1**	Chi-sq = 67.19, d.f. = 2, *P*-value < 0.0001
	Tools with multiple DIF	**11**	**14.7**	**15**	**20.0**	**1**	**1.5**	Chi-sq = 15.96 d.f. = 2, *P*-value = 0.0003
Post-Necsa (sample = 21 pieces)	Step terminating	1	1.02	2	1.46	1	1.8	
	UF spin-off < 6 mm	0	0.00	0	0.00	4	7.0	
	UF spin-off > 6 mm	4	4.08	0	0.00	0	0.0	
	Impact burination	0	0.00	1	0.73	1	1.8	
	Ventral DIF	**5**	**9.4**	**3**	**3.6**	**6**	**35.3**	
	Tools with multiple DIF	**1**	**1.3**	**2**	**2.7**	**2**	**2.9**	
Combined	Step terminating	38	38.78	31	22.63	8	14.0	Chi-sq = 32.02, d.f. = 7, *P*-value < 0.0001
	BF spin-off	2	2.04	14	10.22	0	0.0	
	UF spin-off < 6 mm	4	4.08	7	5.11	11	19.3	
	UF spin-off > 6 mm	5	5.10	18	13.14	0	0.0	
	Impact burination	6	6.12	19	13.87	4	7.0	
	Hinge/feather term.	1	1.02	0	0.00	4	7.0	
	Notch	20	20.41	13	9.49	8	14.0	
	Snap	20	20.41	37	27.01	22	38.6	
	Tools with DIF	**34**	**45.3**	**55**	**73.3**	**17**	**25.0**	
	Ventral DIF	**50**	**86.2**	**60**	**66.3**	**21**	**22.1**	Chi-sq = 98.5, d.f. = 2, *P*-value < 0.0001
	Tools with multiple DIF	**12**	**16.0**	**17**	**22.7**	**3**	**4.4**	Chi-sq = 12.20 d.f. = 2, *P*-value = 0.0022

to and post the micro-XCT scanning. We begin by discussing the macro-fracture results prior to the Necsa scans. A total of 153 DIFs were recorded on the quartz backed tools in the initial macro-fracture analysis (Fig. 2). Fractures on the three functional categories (arrowheads, spear heads, barbs) differed significantly in terms of their pattern and the overall frequency of DIFs (*P* < 0.0001, Table 1). Spear barbs showed a significantly lower DIF frequency (25%) than either arrowheads (45%) or spearheads (73%). Spearheads showed the highest DIF frequencies, confirming the findings of previous hunting experiments (e.g. Fischer *et al.* 1984). Step-terminating bending fractures were the most commonly occurring fracture type on the arrowheads (37%), spearheads (21%) and spear barbs (12%). Unifacial spin-off fractures < 6 mm were noted on all
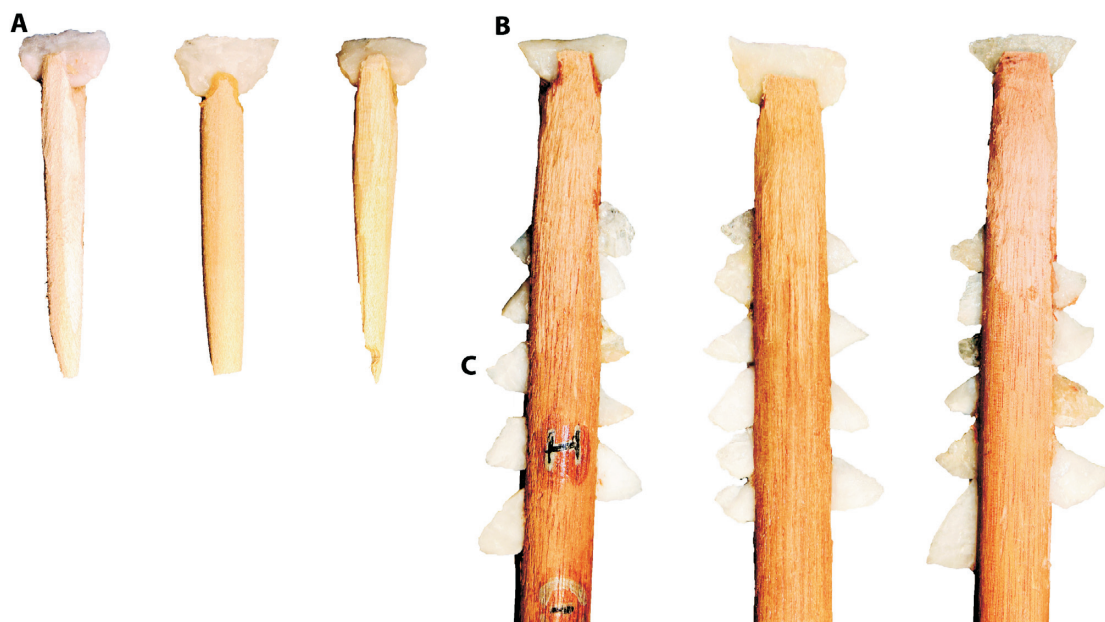
FIG. 1. *Experimental populations;* (**A**) *arrowheads,* (**B**) *spearheads and* (**C**) *spearbarbs.*
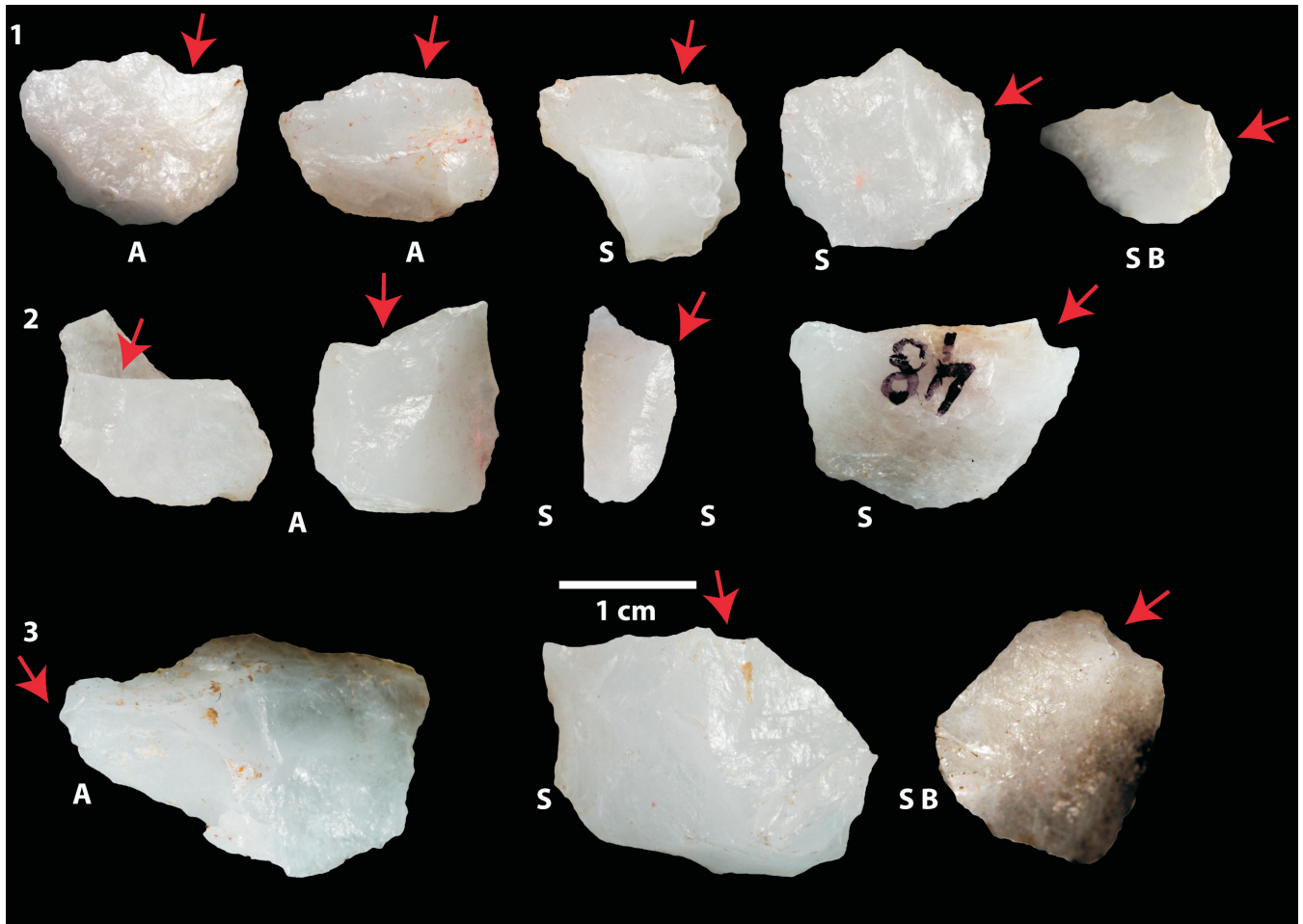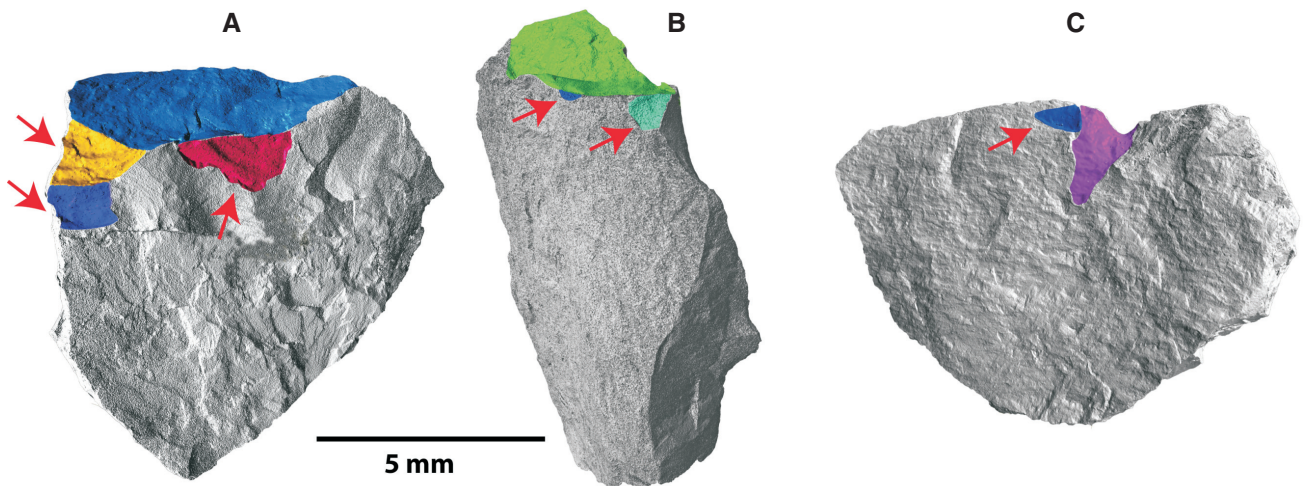
FIG. 2. *Impact fractures on quartz backed tools. (**1**) step-terminating bending fractures; (**2**) spin-off fractures; (**3**) impact burinations. (**A**) arrowheads, (**S**): spearheads, (**SB**) spear barbs. Red arrows indicate direction of fracture formation.*

three weapon categories with the highest frequencies occurring on spear barbs (13.7%). Both unifacial spin-off fractures > 6 mm and impact burinations were recorded in the highest frequencies on spearheads, with only impact burinations noted on the spear barbs (5.3%). These data show that spear barbs accumulate DIFs to a lesser degree than arrow- or spearheads – probably because about half of a backed tool used as a barb inset is embedded in the wooden shaft, protecting its surface from fracturing. Similar experiments, examining the

frequency of DIFs on hafted arrow barbs also resulted in lower DIF frequencies compared to arrowheads (Yaroshevich *et al.* 2010).

Using 3D data obtained with the micro-XCT technique, we discovered 14 additional DIFs on our quartz sample that were not detected during the initial, conventional, macrofracture analysis (Pargeter *et al.* 2016; Fig. 3). These fractures were documented on three arrowheads, two spearheads and two spear barbs. Collectively, they represent an increase of

FIG. 3. *Micro-CT scans showing additional impact fractures. (**A** & **C**) unifacial spin-off fractures; (**B**) step-terminating bending fracture. Red arrows locate fractures.*

TABLE 2. *Overview of DIFs found on the 21 scanned quartz backed tools. Asterisks (*) represent DIFs found on the 3D scans. Ufso: Unifacial spin-off fracture.*

#	Use	Fracture type	2D area	3D area
19	Arrowhead	Step Termination	15.29	17.79
19	Arrowhead	Step Termination	10.68	10.51
19 *	Arrowhead	Ufso > 6 mm	NA	1.87
19 *	Arrowhead	Ufso > 6 mm	NA	1.88
19 *	Arrowhead	Ufso > 6 mm	NA	0.94
20	Arrowhead	Step Termination	7.18	8.33
20	Arrowhead	Step Termination	11.69	16.18
32	Arrowhead	Step Termination	5.88	15.16
32	Arrowhead	Step Termination	11.14	24.40
47	Spearhead	Ufso > 6 mm	1.13	3.80
47 *	Spearhead	Step Termination	NA	11.56
47 *	Spearhead	Impact Burination	NA	8.92
64 *	Arrowhead	Step Termination	NA	5.69
64	Arrowhead	Step Termination	11.80	5.99
68	Spear Barb	Ufso < 6 mm	2.37	10.09
68	Spear Barb	Impact Burination	1.89	9.13
81	Arrowhead	Impact Burination	8.93	13.07
81	Arrowhead	Step Termination	9.04	15.22
91	Arrowhead	Step Termination	21.74	26.63
118	Spearhead	Step Termination	34.77	41.96
121	Arrowhead	Step Termination	4.39	8.37
133	Arrowhead	Ufso > 6 mm	27.68	30.17
133 *	Arrowhead	Ufso > 6 mm	NA	53.55
133	Arrowhead	Impact Burination	9.53	13.31
134 *	Spear Barb	Step Termination	NA	8.99
134 *	Spear Barb	Ufso < 6 mm	NA	0.14
134	Spear Barb	Ufso < 6 mm	1.52	0.68
136	Arrowhead	Step Termination	8.22	11.16
136	Arrowhead	Step Termination	4.21	9.42
138	Spear Barb	Ufso < 6 mm	4.72	3.72
138 *	Spear Barb	Ufso < 6 mm	NA	2.63
138 *	Spear Barb	Ufso < 6 mm	NA	0.98
138 *	Spear Barb	Impact Burination	NA	2.17
138 *	Spear Barb	Ufso < 6 mm	NA	0.60
150 *	Spearhead	Step Termination	NA	2.72
150	Spearhead	Ufso < 6 mm	10.22	9.05
175	Spearhead	Step Termination	12.66	23.35
178	Arrowhead	Step Termination	12.87	16.41
178	Arrowhead	Step Termination	9.90	14.36
180	Spearhead	Ufso > 6 mm	42.06	71.20
185	Arrowhead	Step Termination	13.22	22.88
187	Arrowhead	Step Termination	7.84	15.03
190	Arrowhead	Step Termination	7.56	14.35

c. 33% compared to the previous DIF count ($n = 29$) on the same 21 tools (Tables 1 & 2). The newly observed fractures include eight unifacial spin-off fractures, four step-terminating bending fractures, and two impact burinations. Our observations demonstrate that 3D data are useful for recording small, difficult to detect, secondary fracture types, such as spin-off fractures that form around the periphery of larger, primary DIFs (e.g. step-terminating bending fractures). Spin-offs are widely considered to be the most diagnostic macro-fracture types (see Fisher *et al.* 1984; Pargeter *et al.* 2016). The addition of these new DIFs does not significantly alter the originally recorded DIF patterning, with the three functional categories remaining significantly different in terms of their DIF frequencies ($P < 0.0001$, Table 1). Diagnostic impact fracture frequencies on quartz tools used to tip weapons remained significantly higher than those that developed on the tools used as barbs. Quartz tools used as spearheads showed higher DIF frequencies than those used to tip arrows.

In all cases, we recorded the 3D-detected DIFs in association with already-recorded DIF scars. They reinforce the observation that tools used to tip and barb hunting weaponry are more likely to develop multiple and co-occurring DIFs than tools broken in other, non-hunting scenarios (see Pargeter 2013). Although the addition of the 3D-detected DIFs did not change the significant differences between the three functions in terms of multiple DIF frequencies, it did change the degree of significance. Spear barbs showed the greatest frequency increase of multiple co-occurring DIFs, from 1.5% to 4.4%. These changes brought the three weapons categories closer together and shifted their degree of difference (an order of magnitude) from $P = 0.0003$ prior to scanning, to $P = 0.0022$ after the micro-XCT scanning. Despite these changes, pieces used to tip spears still displayed the highest frequencies of multiple co-occurring DIFs (22.7%) compared to arrowheads (16%) (Table 1).

We calculated the 3D area of all the identified fractures to test for differences in measurement results gained pre- and post-micro-XCT scanning (Fig. 4). First, we outlined the identified fractures by creating 3D surface determinations using the VGStudioMAX™ software. These surfaces were then rendered to provide accurate 3D surfaces from which area measurements could be obtained (Fig. 4). Table 2 and Fig. 5 present the comparative results of our previous 2D and new 3D area measurements. As expected, DIF areas increased in size after being measured on the 3D surfaces, which contain greater topographic detail. Despite this adjustment, the two datasets (2D *vs* 3D area) are not significantly different in this regard ($P = 0.4803$).

To assess whether the changes in area measurements on the 2D and 3D surfaces would affect the relationship between DIF areas and hunting weapon type, we plotted and compared these two sets of area measurements for the three backed tool functional categories. Observations made prior to micro-XCT scanning, showed spearheads to have significantly larger DIF areas than arrowheads (Pargeter *et al.* 2016). Both of these populations had significantly larger DIF areas than the spear barbs (Fig. 5), even though the backed tools were all similar in size.

In Fig. 6 we show the data distributions for the 2D and 3D fracture areas on spearheads, spear barbs and arrowheads prior to and after scanning. There are significant differences between the DIF areas associated with the three backed tool samples using both 2D and 3D surface measurements. These differences shift marginally from $P = 0.0191$ with the 2D measurements, to $P = 0.0183$ with the 3D measurements, but overall they remain statistically significant. A notable change is that data obtained after micro-XCT scanning no longer display statistically different ($P = 0.2817$) DIF areas between spearheads and arrowheads. Our spearhead DIF sample is, however, small (2D areas $n = 5$; 3D areas $n = 7$), thus these results require future assessment with larger sample sizes.

A subsidiary benefit of the micro-XCT technique is that it revealed possible micro-fracture features that are otherwise undetectable on quartz. For example, we observed six possible fracture wings (in 13% of the recorded DIFs) and three possible MLITs (in 6% of the recorded DIFs) on the quartz backed tools (Fig. 7 and Table 2). The features that we tentatively interpret as wings were found within three arrowhead and three spear barb DIFs, while the possible MLITs were found within DIFs on two arrowheads and one spearbarb. Step-terminating bending fractures showed the highest number of fracture wings ($n = 5$), followed by unifacial spin-off fractures < 6 mm ($n = 1$). The MLITs were equally spread between a step-terminating
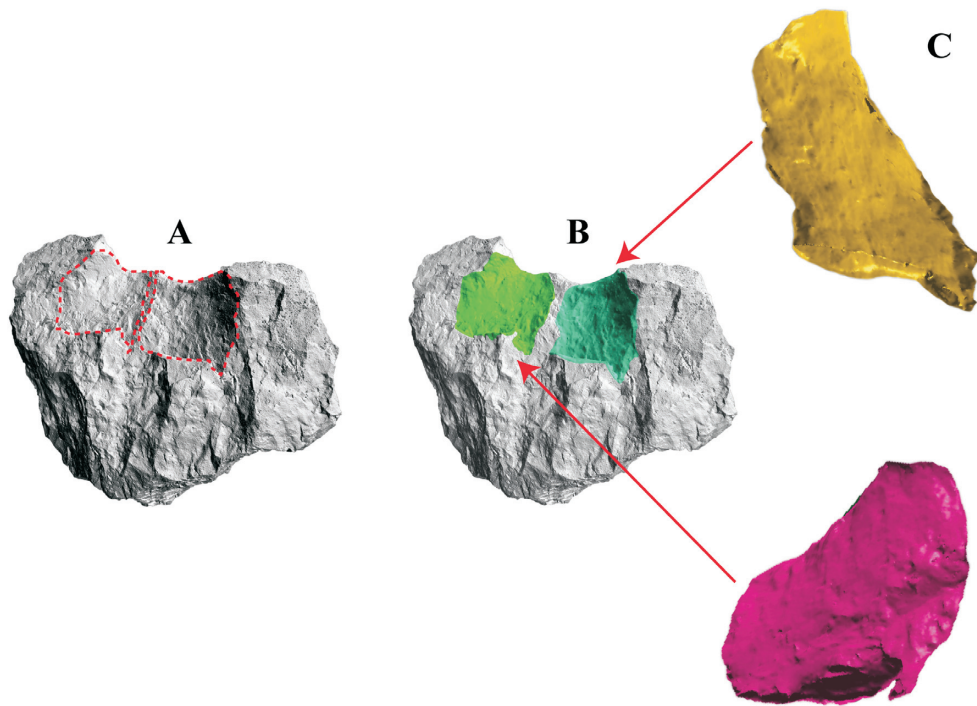
FIG. 4. *Procedure for calculating the area of impact fractures on micro-CT scans.* (**A**) *Outlining relevant fractures.* (**B**) *Create regions of interest for extraction.* (**C**) *Measure extracted surface.*

bending fracture, an impact burination and unifacial spin-off fractures < 6 mm. All of the suggested wings and MLITs were found in an orientation aligned with the major axis of fracture formation, confirming their application for determining the direction of impact. To the best of our knowledge, this is the first instance of what could be interpreted as fracture wings and MLITs being recorded on quartz artefacts used in an experimental hunting context. In the context of this study, our focus was only to assess whether micro-XCT could, in addition to adding value to macro-fracture interpretations, be used to detect these micro-fracture features. Now that we have established this possibility, future work will be conducted which improves on the potential detection of micro-fracture features.

CONCLUSIONS

We have demonstrated the possibilities and advantages of micro-XCT scanning as a new, non-destructive method for analysing replicated quartz artefacts used to tip or barb experimental hunting weaponry. Micro-XCT scanning allows for more accurate macro-fracture description and quantification on quartz than traditional methods using a hand-lens. It is also superior to most microscopy techniques on quartz as the method relies on X-rays instead of light reflectance. The data gained through the scans enable more accurate DIF identifications, a more robust means of measuring the areas of these DIFs, and a possible means of identifying micro-fracture features within these fractures. Further scanning is necessary to verify the identity of these possible micro-fracture features.
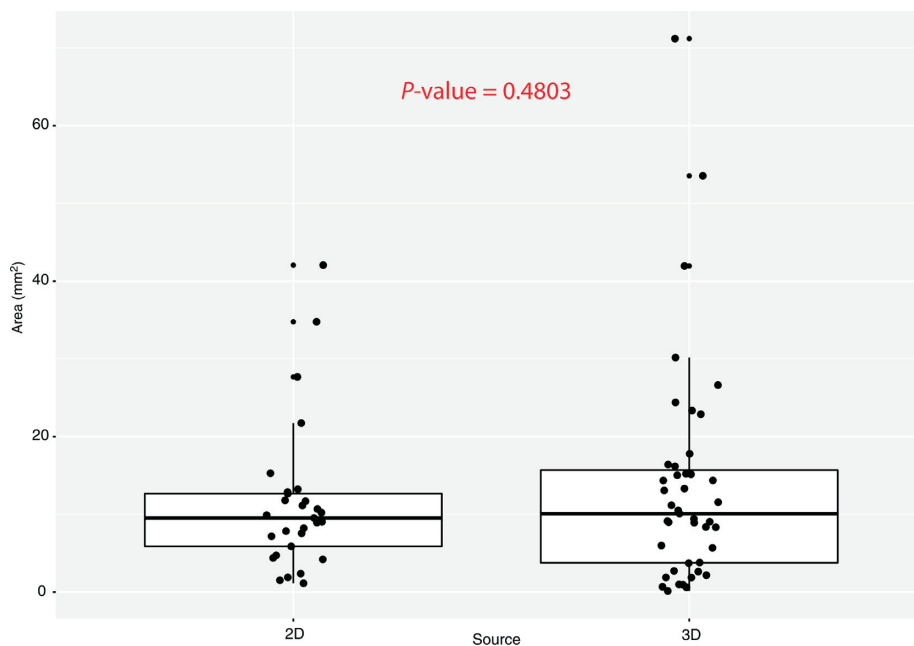
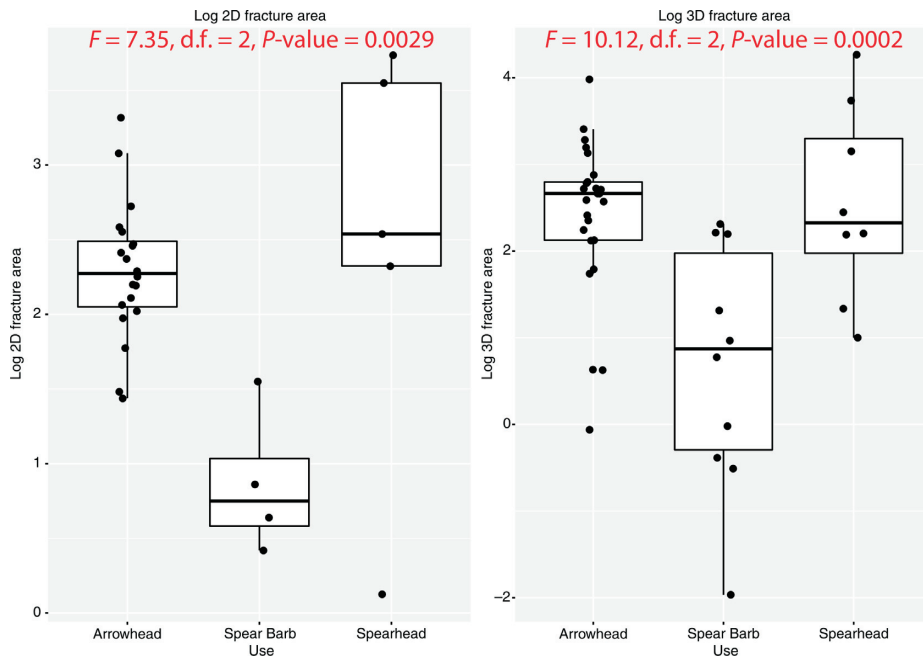**FIG. 5**. *Data distributions for 2D and 3D impact fracture areas.*

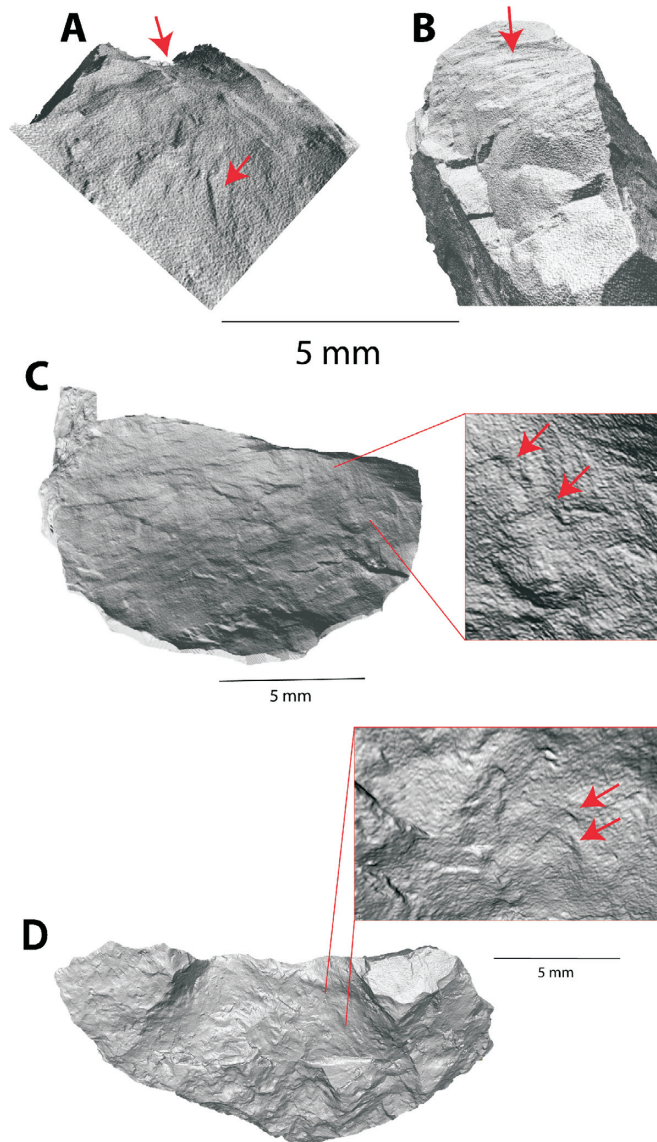**FIG. 6**. *Data distributions for 2D and 3D DIF areas.*

FIG. 7. *Micro-CT scans with possible MILTs and fracture wings indicated. (**A**) Impact burination on arrowhead. (**B**) Step-terminating bending fracture on arrowhead. (**C**) Unifacial spin-off fracture > 6 mm on arrowhead. (**D**) Step-terminating bending fracture on arrowhead.*

The macro-fracture method remains one of the most robust means of assessing the impact function, such as hunting, of stone artefacts. However, there are a number of issues with how the method is implemented and with how its most typical traces, DIFs, are identified, characterised, and quantified. These problems are especially prevalent on artefacts made of quartz given its light reflective properties and anisotropic crystal structure. This is a major problem because numerous archaeological assemblages in Africa and around the world include quartz stone artefacts (e.g. Flenniken 1981; Callahan 1987; Driscoll 2010; Cornelissen 2016). Some of these assemblages feature in debates about prehistoric weapons (e.g. Nassaney & Pyle 1999; Roberts *et al.* 2015), which suggests a wider application for the micro-XCT method and results reported on here.

Now that we have established the usefulness of micro-XCT scanning for characterising macro-fracture scars, the next phase of our exploration will involve applying this method to archaeological assemblages. Scanning some of the Sibudu quartz pieces previously suggested as arrow tips, might strengthen or constrain that interpretation. Lombard and Phillipson (2010) have also questioned whether quartz pieces from Umhlatuzana dating to more than 60 ka functioned as arrows tips. The assemblage from this site contains relatively large numbers of quartz backed tools throughout its sequence, dating from more than 70 ka to the Holocene (Kaplan 1990; Lombard *et al.* 2010). Analysing samples of backed quartz pieces through time with the micro-XCT method may reveal variation in hunting systems for which these tools were used.

ACKNOWLEDGEMENTS

REFERENCES

Callahan, E. 1987. *An Evaluation of the Lithic Technology in Middle Sweden During the Mesolithic and Neolithic*. Upsalla: Societas Archaeologica Upsaliensis.

Cnudde, V. & Boone, M.N. 2013. High-resolution X-ray computed tomography in geosciences: a review of the current technology and applications. *Earth-Science Reviews* 123: 1–17.

Cornelissen, E. 2016. The later Pleistocene in the northeastern Central African rainforest. In: Jones, S. & Stewart, B.A. (eds) *Africa from MIS 6-2: Population Dynamics and Paleoenvironments*: 301–319. Dordrecht: Springer.

Dockall, J.E. 1997. Wear traces and projectile impact: a review of the experimental and archaeological evidence. *Journal of Field Archaeology* 24: 321–331.

Driscoll, K. 2010. Understanding quartz technology in early prehistoric Ireland. Unpublished PhD thesis. Dublin: University College Dublin.

Eren, M.I., Lycett, S.J., Patten, R.J., Buchanan, B., Pargeter, J. & O'Brien, M.J. 2016. Test, model, and method validation: the role of experimental stone-tool replication in hypothesis-driven archaeology. *Ethnoarchaeology* 8: 103–136.

Fischer, A., Hansen, P.V. & Rasmussen, P. 1984. Macro and micro wear traces on lithic projectile points: experimental results and prehistoric examples. *Journal of Danish Archaeology* 3: 19–46.

Flenniken, J.J. 1981. *Replicative Systems Analysis: A Model Applied to the Vein Quartz Artifacts from the Hoko River Site*. Pullman: Washington State University Laboratory of Anthropology Reports of Investigation.

Geneste, J.M. & Plisson. H. 1990. Technologie fonctionelle des pointes a cran Solutréennes: l'apport des nouvelles données de la grotte de Combe Saunière (Dordogne). In: Kozlowski, J (Ed.) *Les Industries à pointes foliacées du Paléolithique supérieur européen*: 293–320. Liège: ERAUL.

Hoffman, J.W. & De Beer, F. 2012. Characteristics of the micro-focus x-ray tomography facility (MIXRAD) at Necsa in South Africa. *18th World Conference on Nondestructive Testing*, 16–20.

Hutchings, K.W. 2016. When is a point a projectile? Morphology, impact fractures, scientific rigor, and the limits of inference. In: Iovita, R. & Sano, K. (eds) *Multidisciplinary Approaches to the Study of Stone Age Weaponry*. Dordrecht: Springer.

Iovita, R. & Sano, K. 2016. *Multidisciplinary Approaches to the Study of Stone Age Weaponry*. Dordrecht: Springer.

Iovita, R., Schönekeß, H., Gaudzinski-Windheuser, S. & Jäger, F. 2016. Identifying weapon delivery systems using macrofracture analysis and fracture propagation velocity: a controlled experiment. In: Iovita, R. & Sano, K. (eds) *Multidisciplinary Approaches to the Study of Stone Age Weaponry*: 13–27. Dordrecht: Springer.

Kaplan, J.M. 1990. The Umhlatuzana Rock Shelter sequence: 100 000 years of Stone Age history. *Natal Museum Journal of Humanities* 2: 1–94.

Lombard, M. 2005. A method for identifying Stone Age hunting tools. *South African Archaeological Bulletin* 60: 115–120.

Lombard, M. 2011. Quartz-tipped arrows older than 60 ka: further use-trace evidence from Sibudu, KwaZulu-Natal, South Africa. *Journal of Archaeological Science* 38: 1918–1930.

Lombard, M. & Pargeter, J. 2008. Hunting with Howiesons Poort segments: pilot experimental study and the functional interpretation of archaeological tools. *Journal of Archaeological Science* 35: 2523–2531.

Lombard, M. & Phillipson, L. 2010. Indications of bow and stone-tipped arrow use 64 000 years ago in KwaZulu-Natal, South Africa. *Antiquity* 84: 635–648.

Lombard, M., Wadley, L., Jacobs, Z., Mohapi, M. & Roberts, R. 2010. Still Bay and serrated points from Umhlatuzana, KwaZulu-Natal, South Africa. *Journal of Archaeological Science* 37: 1773–1784.

Nassaney, M.S. & Pyle, K. 1999. The adoption of the bow and arrow in eastern North America: a view from central Arkansas. *American Antiquity* 64: 243–264.

Pargeter, J. 2013. Rock type variability and impact fracture formation: working towards a more robust macrofracture method. *Journal of Archaeological Science* 40: 4056–4065.

Pargeter, J., Shea, J., Utting, B., 2016. Quartz backed tools as arrowheads and hand-cast spearheads: hunting experiments and macro-fracture analysis. *Journal of Archaeological Science* 73: 145–157.

Phillipson, L. 2009. *Using Stone Tools: the Archaeological Evidence from Aksum, Ethiopia*. Oxford: Archaeopress.

Roberts, P., Boivin, N. & Petraglia, M. 2015. The Sri Lankan 'microlithic' tradition c. 38,000 to 3,000 years ago: tropical technologies and adaptations of *Homo sapiens* at the southern edge of Asia. *Journal of World Prehistory*: 1–44.

Rots, V. & Plisson, H. 2013. Projectiles and the abuse of the use-wear method in a search for impact. *Journal of Archaeological Science* 48: 154–165.

Sano, K., Denda, Y. & Oba, M. 2016. Experiments in fracture patterns and impact velocity with replica hunting weapons from Japan. In: Iovita, R. & Sano, K. (eds) *Multidisciplinary Approaches to the Study of Stone Age Weaponry*: 29–46. Dordrecht: Springer.

Sisk, M.L. & Shea, J.J. 2009. Experimental use and quantitative performance analysis of triangular flakes (Levallois points) used as arrowheads. *Journal of Archaeological Science* 36: 2049–2047.

Wadley, L. & Mohapi, M. 2008. A segment is not a monolith: evidence from the Howiesons Poort of Sibudu, South Africa. *Journal of Archaeological Science* 35: 2594–2605.

Yaroshevich, A., Kaufman, D., Nuzhnyy, D., Bar-Yosef, O. & Weinstein-Evron, M. 2010. Design and performance of microlith implemented projectiles during the Middle and the Late Epipaleolithic of the Levant: experimental and archaeological evidence. *Journal of Archaeological Science* 37: 368–388.